Effect of pressure and temperature on electronic structure of GaN in the zinc-blende structure

© A.R. Degheidy¶, E.B. Elkenany

Department of Physics, Faculty of Science, Mansoura University,
35516 Mansoura, Egypt

(Получена 12 января 2011 г. Принята к печати 22 марта 2011 г.)

The effect of the hydrostatic pressure and the temperature on the electronic structure in GaN semiconductor has been calculated using the local empirical pseudopotential method. The variation of the direct and indirect energy gaps with the pressure up to 120 kbar and with the temperature up to 500 K has been done. The calculated fundamental energy gap at different pressures and different temperatures are calculated and compared with the available experimental data which show excellent agreement. The effect of pressure and temperature on the refractive index of the considered materials has also been studied.

1. Introduction

From 15 years ago, in many laboratories of Germany, Japan, USA, Russia, Poland, China, and other countries, intensive theoretical and experimental studies of nitrides of Group III elements (GaN, AlN, InN) in the form of single crystals, thin films, alloys, and heterosturctures on their basis have been carried out [1]. $A^{III}B^{V}$ nitride semiconductors have attracted much attention for their potential use in optoelectronic device applications [2–4]. The large interest originates from their promising potential for shortwavelenght light-emitting diodes, semiconductor lasers and optical detectors, as well as for high-temperature, high-power, and high-frequency devices [5]. GaN is one of the $A^{III}B^{V}$ nitride wide-band gap semiconductors. It is of particular interest because it has high electron mobility as compared to other wide-band gap electronic materials. It is also characterized by having high hardness, low compressibility, high ionicity, and high thermal conductivity. Such properties make it a good candidate for optoelectronic devices operating under extreme conditions [6].

Takahiro Maruyama et al. were investigated the valence band structures of both wurtzite and zinc blende GaN by angle resolved photoemission spectroscopy [7]. V.N. Brudnyi et al. were calculated the electronic spectra and the energy position of the local charge-neutrality level for the wurtzite BN, AlN, GaN, and InN compounds with use of different heuristic models [8]. L. Wenchang et al. were studied the ground-state properties, band structures and pressure dependence of the band gaps of zinc blende GaN by the linear muffin-tin orbital method with the atomic-sphere approximation [9]. Masakatsu Suzuki et al. were calculated the electronic band structure for wurtzite-type GaN by using a full-potential linearized augmented plane wave (FLAPW) method [10]. The studies of the pressure and temperature dependences of optoelectronic properties in semiconductors can provide additional valuable information about the electronic band structure and optical properties. Since the essential transport mechanisms are tightly bound to their band gaps, so the knowledge of this latter and its behavior under pressure and temperature would enable us to predict the overall properties of these materials. In the present study, we reported on the influence of pressure and temperature on the electronic band structures of semiconductor GaN more specifically on the energy band gaps at Γ, X and L high-symmetry points. These effects have been predicted by computing the changes of the form factors and the lattice constant, and consequently the electronic band structure of GaN with changes in pressure and temperature. We also showed the effect of pressure and temperature on the variation of the electronic energy band $E_{nk}(P)$ and $E_{nk}(T)$ as functions of the wave vector $\mathbf{k}$ of the Brillouin zone.

The calculations in this work involved the local empirical pseudopotential method (EPM) but ignore the non-local and spin-orbit corrections. In the local EPM, the core electrons are tightly bound to their nuclei and the valence electrons are influenced only by a weak net effective potential, i.e. the large attractive core potential energy of the ion core is cancelled by the large positive kinetic energy of the electron due to its rapid oscillations [11–15]. In the non-local EPM the pseudopotential depends on the orbital angular momentum parameter of the atomic core states, which is ignored in the local calculations [15–17]. In spin-orbit calculations, the degeneracy of the valance band maxima is lifted [18–20].

2. Theory and calculations

Employing the local EPM method, the eigenvalues $E_{nk}(P)$ and $E_{nk}(T)$ are calculated by solving numerically the matrix equation

$$\frac{\hbar^2}{2m}|\mathbf{k}+\mathbf{G}'|^2 A_{n,\mathbf{k}}(\mathbf{G}',X) + \sum_{G\neq G'} A_{n,\mathbf{k}}(\mathbf{G}',X)V^l(|\mathbf{G}-\mathbf{G}'|,X) = E_{nk}(X)A_{n,\mathbf{k}}(\mathbf{G}',X) \quad (1)$$

where

$$V^l(\mathbf{G}-\mathbf{G}',X) = W^s(\Delta\mathbf{G},X)\cos(\Delta\mathbf{G}\cdot\boldsymbol{\tau}) + iW^a(\Delta\mathbf{G},X)\sin(\Delta\mathbf{G}\cdot\boldsymbol{\tau}) \quad (2)$$

is the X-dependent pseudopotential and X means the pressure P or the temperature T. $W^{s,a}(\Delta\mathbf{G},X)$ are the

¶ E-mail: ardegheidy@mans.edu.eg,
kena@mans.edu.eg

symmetric (W^s) and anti-symmetric (W^a) X-dependent form factors that are fitted empirically to obtain the required energy gap for the associated semiconductor. $\mathbf{G}$ and $\mathbf{G}'$ are the reciprocal lattice vectors, with $\Delta\mathbf{G} = \mathbf{G} - \mathbf{G}'$ and $\tau = \frac{a(X)}{8}(1,1,1)$, is the position vector of each atom in the unit cell and $a(X)$ is the X-dependent lattice constant.

Applying the atomic units, $e = m = \hbar = 1$, Eq. (1) can be rewritten as

$$\left\| \frac{1}{2} |\mathbf{k} + \mathbf{G}'|^2 - E_{nk}(X) + \sum_{\mathbf{G}\neq\mathbf{G}'} V_p^l(|\mathbf{G} - \mathbf{G}'|, X) \right\| = 0. \quad (3)$$

The first two terms in the above equation, Eq. (3) constitute the diagonal elements of the matrix, while the third term constitutes the off-diagonal elements. The $\mathbf{k}$ values are chosen by considering a specimen of length $50a(X)$, so the number of sampling points is twice the value of 50 by considering the whole interval of the Bz $[-1, 1]$. So, one obtains the incrimination $\Delta\mathbf{k}$ of $\mathbf{k}$, in units of $\pi/a(X)$ [21].

To solve Eq. (3) numerically, we use our own routine based on the MATLAB language [22], which is 65×65 matrix based on 65 bulk reciprocal lattice vectors, $\mathbf{G}'s$. These values are corresponding to $|\Delta\mathbf{G}|^2 = 3$, 4 and 11 for zinc-Blende type structure, which satisfy the condition $|\Delta G|^2 \leq 11$, that gives non-zero pseudopotential. The $\mathbf{G}$'s values are listed in Refs [21,23].

Arranging the calculated eigenvalues descendingly to obtain the valence and conduction bands. Set the top of the valence bands to zero energy and determine the energy gaps. The best values of energy gaps can be obtained by adjusting the form factors until the determined energy gaps match the corresponding experimental values.

The refractive index of GaN at different pressures and different temperatures are calculated by using the three models found in Ref [24–26].

3. Results and discussion

3.1. Pressure dependence at room temperature

The pressure dependent energy levels, $E_{nk}(P)$, at different $\mathbf{k}$ values are obtained by solving the secular determinant (3) with $X = P$

$$\left\| \frac{\hbar^2}{2m} |\mathbf{k} + \mathbf{G}'|^2 - E_{nk}(P) + \sum_{\mathbf{G}\neq\mathbf{G}'} V^l(|\mathbf{G} - \mathbf{G}'|, P) \right\| = 0. \quad (4)$$

The experimental pressure dependent energy gaps are obtained from the empirical relation [27],

$$E_g^{\mathrm{d,id}}(P) = E_g^{\mathrm{d,id}}(0) + aP + bP^2,$$

where a and b are the hydrostatic pressure coefficients listed in Table 1, ″d″ and ″id″ stand for direct and indirect energy bands.

Table 1. Values of the bulk modulus B, and its pressure derivative B', the hydrostatic pressure parameters a and b; values of the Varshni's parameters[a] and the linear thermal expansion coefficients[a] for GaN zinc blende semiconductor

GaN			
Hydrostatic pressure parameter [a]		Varshni's parameters [b]	
a (10^{-3} eV/kbar)	4.2		
b (10^{-5} eV/kbar^2)	−1.8	$\alpha(10^{-4}\,\mathrm{K}^{-2})$	7.7
B (GPa)	200	β(K)	600
B'	4.4	$\alpha_{\mathrm{th}}(10^{-6}\,\mathrm{K}^{-1})$	5.497

Note. [a]Ref. [27];
[b]Ref. [28].

$W^{s,a}(\Delta\mathbf{G}, P)$ are the pressure-dependent form factors that are fitted empirically with the experimental values to obtain the required energy gap for the associated semiconductor and take the form

$$W^{s,a}(\Delta\mathbf{G}, P) = W^{s,a}(\Delta\mathbf{G}, P = 0) + \Delta^{s,a}P, \quad (5)$$

where $\Delta^{s,a}$ are the pressure coefficient form factors.

The pressure dependence lattice constant has been estimated using the relation given by Adachi [27].

$$a(P) = a(0)\left[1 + \left(\frac{B'}{B}\right)P\right]^{-1/3B}, \quad (6)$$

where B is the bulk modulus, and B' is the pressure derivative of the bulk modulus which are listed in Table 1. $a(0)$ and $a(P)$ are the lattice parameters at pressures $P = 0$ and $P \neq 0$, respectively.

Table 2 shows the adjusted local symmetric and antisymmetric pseudopotential form factors at different values of $|\Delta\mathbf{G}|^2$ for GaN, together with its lattice constant at various pressure values from zero to 120 kbar.

It is seen that W_{11}^s, W_4^a are more sensitive to the pressure than the others. They are linearly increasing functions with increasing the pressure.

The fundamental energy gaps at different pressures are also found in table 2 which shows excellent agreement with the experimental data [27].

In Fig. 1 we show the calculated energy band structure of GaN at zero pressure (solid lines) and at 120 kbar pressure (dashed lines). It is seen from Fig. 1 that the energy differences between the calculated electronic energies at 0 kbar and 120 kbar are bout 268.7 meV at the X-point, 98 meV at the L-point and 244.9 meV at Γ-point. At zero pressure the minimum of the conduction band is at the high-summetry point Γ. Hence, GaN is a direct-gap ($\Gamma-\Gamma$) semiconductor. When the pressure increasing, the first conduction band at Γ and L points shift upwards, while at the X-point the first conduction band moves slightly down relative to the valence-band maximum. This makes the minimum of the first conduction band is at the X-point.

Table 2. The adjusted local symmetric form factors, lattice constant, and the fundamental energy gaps for GaN at various values of pressure at room temperature.

Form factors (a.u.)	$\Delta^{s,a}$, 10^{-6} (kbar^{-1})	P(kbar)				
		0	30	60	90	120
$W_3^s(P)$	0.0417000	−0.2513150	−0.2513167	−0.2513155	−0.2513142	−0.2513129
$W_8^s(P)$	0.0041700	−0.0105325	−0.0105324	−0.0105322	−0.0105321	−0.0105319
$W_{11}^s(P)$	43.7750000	0.1123650	0.1141360	0.1156130	0.1167650	0.1175880
$W_3^a(P)$	0.0041700	−0.0162975	−0.0162973	−0.0162972	−0.0162971	−0.0162969
$W_4^a(P)$	41.6667000	0.1000000	0.1012500	0.10250000	0.1037500	0.1050000
$W_{11}^a(P)$	0.5667000	0.0677320	0.0677490	0.0677660	0.0677830	0.0678000
$a(P)$ (a.u.)		8.5039000	8.4628000	8.4244000	8.3883000	8.3543000
$E_g(P)$ in eV						
Present results		3.2030000	3.3098000	3.3872000	3.4322000	3.4448000
Experimental results		3.2000000 [a]	3.3098000 [a]	3.3872000 [a]	3.4322000 [a]	3.4448000 [a]

Note. [a] Ref. [27].

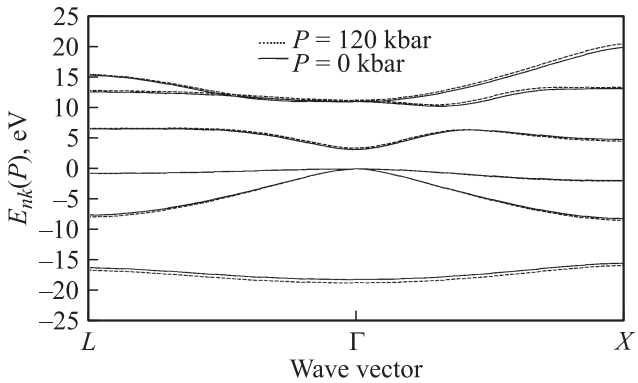

Fig. 1. The energy band structure of GaN at zero pressure (solid lines) and at 120 kbar pressure (dashed lines).

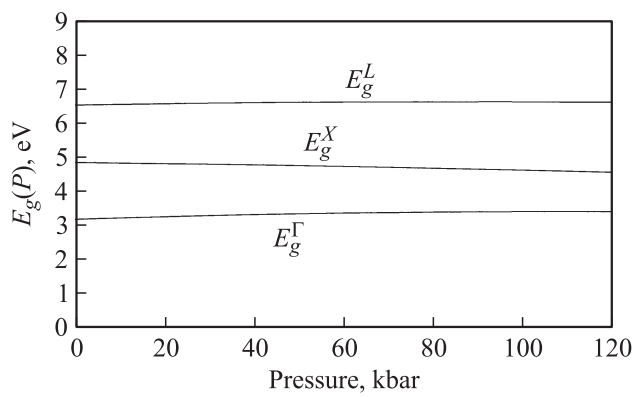

Fig. 2. The direct and indirect energy band gaps as function of pressure for GaN.

Fig. 2 shows the direct and indirect energy band gaps as function of pressure. The direct energy gap E_g^Γ and the indirect band gaps E_g^L are increased by increasing the pressure while the indirect band gap E_g^X is decreased. The dependencies of the direct and indirect band gaps for zincblende GaN on pressure could be also represented by means of quadratic regressions through the equations:

$$E_g^\Gamma = 3.2 + 89.375\left(\frac{\Delta a(P)}{a(P)}\right) - 47633\left(\frac{\Delta a(P)}{a(P)}\right)^2, \quad (7)$$

$$E_g^x = 4.876 + 6.6447\left(\frac{\Delta a(P)}{a(P)}\right) - 7141.7\left(\frac{\Delta a(P)}{a(P)}\right)^2, \quad (8)$$

$$E_g^L = 6.6006 - 17.558\left(\frac{\Delta a(P)}{a(P)}\right) - 9413.1\left(\frac{\Delta a(P)}{a(P)}\right)^2, \quad (9)$$

where $\Delta a(P) = a(P) - a(0)$.

In Fig. 3 the refractive index of GaN is plotted against the pressure using three different models. Herve and Vandamme, Moss and Ravindra's [24–26] relations are empirical relationships have been established for the estimation of refractive indices for various materials directly from their energy gaps. The Moss relation based on an atomic model gives values of refractive index which are larger than those obtained by the two other models. However, the effect of pressure on the refractive index seems to be stronger when using the Ravindra et al. relation. For all models

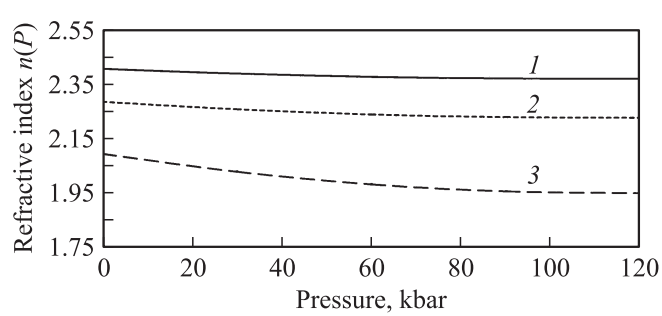

Fig. 3. Refractive index as a function of pressure in GaN calculated by: *1* — the Ravindra et al. relation [25], *2* — the Herve and Vandamme relation [26], *3* — the Moss relation [24].

Table 3. The adjusted local symmetric form factors, lattice constant, and the fundamental energy gaps for GaN at various values of temperature at normal pressure.

Form factors (a.u.)	$\Delta^{s,a}$, 10^{-6} (K^{-1})	T (K)					
		0	100	200	300	400	500
$W_3^s(T)$	0.0066670	−0.2513130	−0.2513136	−0.2513143	−0.2513150	−0.2513157	−0.2513163
$W_8^s(T)$	0.0016667	−0.0105320	−0.0105322	−0.0105320	−0.0105325	−0.0105327	−0.0105328
$W_{11}^s(T)$	3.3533330	0.1133710	0.1131780	0.1128250	0.1123650	0.1118290	0.1112410
$W_3^a(T)$	0.0250000	−0.0162900	−0.0162925	−0.0162950	−0.0162975	−0.0163000	−0.0163025
$W_4^a(T)$	1.6666667	0.1005000	0.1003333	0.1001667	0.1000000	0.0998333	0.0996667
$W_{11}^a(T)$	0.0166670	0.0677370	0.0677353	0.0677337	0.0677320	0.0677303	0.0677286
$a(T)$ (a.u.)		8.4899000	8.4946000	8.4992000	8.5039000	8.5086000	8.5132000
$E_g(T)$ in eV							
Present results		3.2800000	3.2690000	3.2415000	3.2030000	3.1568000	3.1050000
Experimental results		3.2800000 [b]	3.2690000 [b]	3.2415000 [b]	3.2030000 [b]	3.1568000 [b]	3.1050000 [b]

Note. [b] Ref. [28].

used, the refractive index decreases linearly with increasing pressure up to 120 kbar. This fact leads us to believe that the zinc-blende GaN shows that the smaller fundamental energy band gap material has a large value of the refractive index.

Similar to the band gap energies, we can represent as well the pressure variaton of the refractive index for the material of interest through the following equation

$$n_1 = 2.4103 + 1.0918\left(\frac{\Delta a(P)}{a(P)}\right) - 81.978\left(\frac{\Delta a(P)}{a(P)}\right)^2, \quad (10)$$

$$n_2 = 2.1 + 3.5273\left(\frac{\Delta a(P)}{a(P)}\right) - 294.16\left(\frac{\Delta a(P)}{a(P)}\right)^2, \quad (11)$$

$$n_3 = 2.2904 + 1.6244\left(\frac{\Delta a(P)}{a(P)}\right) - 123.62\left(\frac{\Delta a(P)}{a(P)}\right)^3, \quad (12)$$

where n_1, n_2 and n_3 are referred to as refractive indices obtained from relations (10)–(12), respectively.

3.2. Temperature dependence at normal pressure

The temperature dependent eigenvalues $E_{nk}(T)$ are found by solving the secular determinant (3) with $X = T$

$$\left\| \frac{\hbar^2}{2m}|\mathbf{k}+\mathbf{G}'|^2 - E_{nk}(T) + \sum_{\mathbf{G}\neq\mathbf{G}'} V_p^l|\mathbf{G}-\mathbf{G}'|, T) \right\| = 0, \quad (13)$$

$W^{s,a}(\Delta\mathbf{G}, T)$ are the temperature-dependent form factors that are fitted empirically with the experimental values to obtain the required energy gaps for the associated semiconductor. The form factors take the form

$$W^{s,a}(\Delta\mathbf{G}, T) = W^{s,a}(\Delta\mathbf{G}, T = 0\,\mathrm{K}) - \Delta^{s,a}T, \quad (14)$$

where $\Delta^{s,a}$ are the temperature coefficient form factors and $a(T)$ is the temperature-dependent lattice constant, which is determined from the relation [27]

$$a(T) = a(300\,\mathrm{K})[1 + \alpha_{\mathrm{th}}(T - 300\,\mathrm{K})],$$

where α_{th} is the linear thermal expansion coefficient and its value that corresponding to the associated semiconductor is listed in Table 2.

The experimental temperature energy gaps are obtained from Varshni's [28] empirical formula as

$$E_g(T) = E_g(0) - \frac{\alpha T^2}{T+\beta}.$$

The values of α and β for GaN are also listed in Table 1.

The temperature dependent-form factor parameters for GaN as functions of temperature at different values of $|\Delta G|^2$ are listed in Table 3. It is seen from this table that the temperature-dependent from factors are linearly varied with temperature; they are linearly decreasing functions with increasing temperature. This is due to the fact that, raising temperature increases the dimension of the crystal, as observed from the variation of the lattice constant $a(T)$, which yields decreasing the potential energy seen by the electron. Excellent agreement is seen from Table 3 when comparing the calculated fundamental energy gap of GaN, with the experimental data [28].

Table 3 shows that the fundamental energy gaps are more sensitive to the temperature dependent from factor associated with the reciprocal lattice vectors W_{11}^s, W_4^a.

Fig. 4 shows the variation of the temperature dependent electronic energy band structure for GaN as a function of the propagation wave vector $\mathbf{k}$ and temperature $T = 0\,\mathrm{K}$ (solid line) and 500 K (dashed line). It is seen that the temperature dependent first conduction energy band is more affected by temperature than the other conduction and valence bands and exhibits more enhancement at the Γ-point of symmetry than any other k-point in the Brillouin zone. The conduction bands are also more affected by temperatures than the valence bands. The temperature

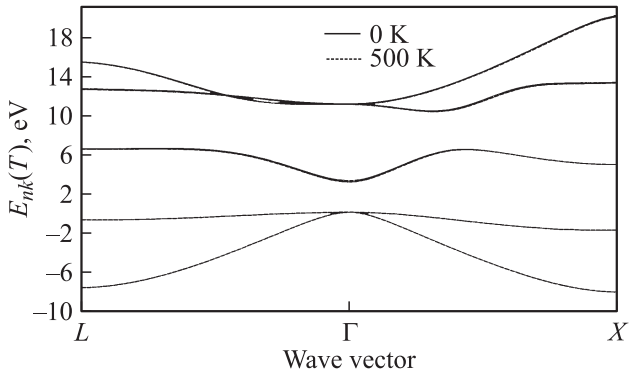

Fig. 4. The energy band structure of GaN at 0 K (solid lines) and at 500 K (dashed lines).

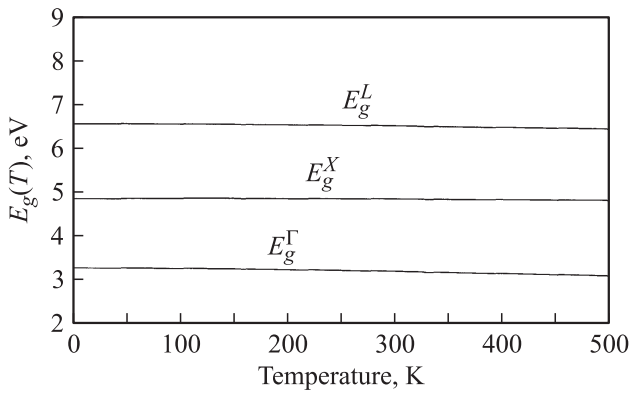

Fig. 5. The direct and indirect energy band gaps as function of temperature for GaN.

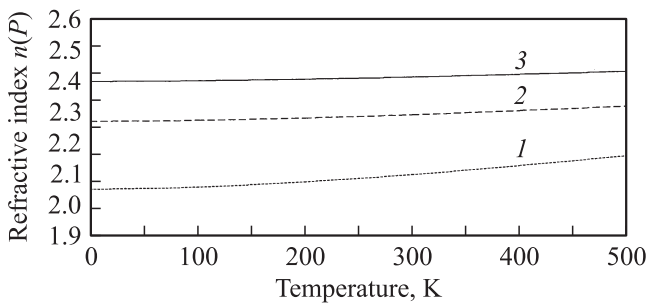

Fig. 6. Refractive index as a function of pressure in GaN calculated by: *1* — the Ravindra et al. relation [25], *2* — the Herve and Vandamme relation [26], *3* — the Moss relation [24].

effect becomes less pronounced for higher conduction bands and nearly most valence bands. The energy differences between the calculated electronic energies at 0 and 500 K are about 175.1 meV at Γ-point, 109.2 meV at the L-point, and 292 meV at the X-point.

The direct and indirect energy band gaps as function of temperature obtained for GaN are plotted in Fig 5. We show that the direct energy gap E_g^Γ and the indirect band gaps E_g^L and E_g^X are decreased by increasing the temperature. The dependencies of the direct and indirect band gaps for zincblende GaN on temperature could be also represented by means of quadratic regressions through the equations:

$$E_g^\Gamma = 3.28 - 16.716\left(\frac{\Delta a(T)}{a(T)}\right) - 17933\left(\frac{\Delta a(T)}{a(T)}\right)^2, \quad (15)$$

$$E_g^x = 4.871 + 13.239\left(\frac{\Delta a(T)}{a(T)}\right) - 8987.9\left(\frac{\Delta a(T)}{a(T)}\right)^2, \quad (16)$$

$$E_g^L = 6.5935 - 8.0852\left(\frac{\Delta a(T)}{a(T)}\right) - 120653\left(\frac{\Delta a(T)}{a(T)}\right)^2, \quad (17)$$

where $\Delta a(T) = a(T) - a(0)$ and $a(T)$ and $a(0)$ are the lattice constants at temperature T and at zero temperature, respectively.

As can be seen from Eqs. (15)–(17), all dependencies show a non-linear behavior. Also, we can represent the temperature variation of the refractive index for the material of interest through the following equation

$$n_1 = 2.3955 - 2.2688\left(\frac{\Delta a(T)}{a(T)}\right) - 3994.4\left(\frac{\Delta a(T)}{a(T)}\right)^2, \quad (18)$$

$$n_2 = 2.2683 - 3.3091\left(\frac{\Delta a(T)}{a(T)}\right) - 5946.1\left(\frac{\Delta a(T)}{a(T)}\right)^2, \quad (19)$$

$$n_3 = 2.0504 - 7.0149\left(\frac{\Delta a(T)}{a(T)}\right) - 13099\left(\frac{\Delta a(T)}{a(T)}\right)^2. \quad (20)$$

In Fig. 6 the refractive index is plotted against temperature using the three different models [24–26]. For all models used, the refractive index increases linearly with increasing temperature up to 500 K.

As expected, the direct energy gaps increases with pressure and decreases with temperature and the effect of pressure on the electronic structure of GaN is more than the effect of temperature.

4. Conclusion

We have performed calculations of the temperature and pressure dependent electronic energy band structures for GaN in the zinc-blende structure based on local empirical pseudopotential method, and ignoring the non-local and the spin-orbin coupling effects. The temperature and pressure dependence of the pseudopotential is performed by considering the temperature and pressure dependence of the lattice constant, and the form factors. The refractive index of the considered material as a function of temperature and pressure is studied. The present electronic band structures calculations show excellent agreements with the experimental data.

Acknowledgements

I am thankful to Prof. A.M. Elabsy for various discussions and help in calculations. Thanks are also due to Prof. E.A. Elwakil of his advising and encouragements. The assistance from University of Mansoura is also achnowledged.

References

[1] T.V. Gorkavenko, S.M. Zubkova, and L.N. Rusina, Semiconductors. 41 (2007) 641–650.
[2] H. Morkoc, S.N. Mohammad. Science, **267**, 51 (1995).
[3] J.W. Orton, C.T. Foxon, Rep. Progr. Phys., **61**, 1 (1998).
[4] S.C. Jain, M. Willander, J. Narayan, R. Van Overstraeten. J. Appl. Phys., **87** 965 (2000).
[5] D. Vogel, P. Kruger, J. Pollmann, Phys. Rev. B, **55**, 12 836 (1997).
[6] T. Lei, T.D. Moustakas, R.J. Graham, Y. He, S.J. Berkowitz, J. Appl. Phys., **71**, 4933 (1992).
[7] TakaHiro Maruyama, Yutaka Miyajima, Kazutaka Hata, Sung Hwan Cho, Katsuhiro Akimoto, Hajime Okumura, sadafumi Yushida, and Hiroo Kato, J. Electronic Materials. 27 (1998) 4.
[8] V.N. Brudnyi, A.V. Kosobutsky, and N.G. Kolin, Semiconductors. 43 (2009) 1271–1279.
[9] L. Wenchang, Z. Kaiming, and Xie Xide, J. Phys.: Condens. Matter 5 (1993) 875.
[10] Masakatsu Suzuki, and Takeshi Uenoyama, J. Appl. Phys. 34 (1995) 3442–3446.
[11] J.C. Philips, L. Klienman, Phys. Rev., **116**, 287 (1959).
[12] M.H. Cohen, V. Heine, Phys. Rev., **122**, 1821 (1961).
[13] B.J. Austin, V. Heine, L.J. Sham. Phys. Rev., **127**, 276 (1962).
[14] M.L. Cohen, T.K. Bergstresser. Phys. Rev., **141** 780 (1966).
[15] J.C. Phillips, K.C. Pandey. Phys. Rev. Lett., **30**, 787 (1976).
[16] K.C. Pandey, J.C. Phillips. Phys. Rev. B, **9**, 1552 (1974).
[17] J.R. CHelikowsky, M.L. Cohen. Phys. Rev. B, **14**, 556 (1976); Phys. Rev. Lett., **31** (1973).
[18] R. Chelikowsky, M.L. Cohen. Phys. Rev. Lett., **32**, 674 (1974).
[19] W. Potz, P. Volg. Phys. Rev. B, **24**, 2025 (1981).
[20] G. Theurich, N.A. Hill. Phys. Rev. B, **64**, 73 106 (2001).
[21] A.M. Elabsy, E.B. Elkenany. Physica. B 405 (2010) 266.
[22] A. Gilat. *MATLAM An Introduction with Application* (J. Wilely & Sons Inc., 2005).
[23] P. Harrison. *Quantum Wells Wires and Quantum Dots* (J, Wiley & Sons Ltd., 2005), 2nd ed., Chap. 11.
[24] V.P. Gupta, N.M. Ravindra. Phys. Status Solidi B, **100**, 715 (1980).
[25] N.M. Ravindra, S. Auluck, V.K. Srivastava. Phys. Status Solidi B, **93**, k155 (1979).
[26] P.J.L. Herve, L.K.J. Vandamme. Infr. Phys. Technol., **35** 609 (1994).
[27] S. Adachi. *Properties of Group IV, III–V and II–VI Semiconductors.* Wiley, N.Y., (2005) chap. 2.
[28] Y.P. Varshni. Physica, **34** 149 (1967).

Редактор Т.А. Полянская